



Measurements of the spectral location of the structured target resonance for ultrarelativistic electrons



K.K. Andersen^{a,*}, S.L. Andersen^a, H. Knudsen^a, R.E. Mikkelsen^a, H.D. Thomsen^a, U.I. Uggerhøj^{a,*}, T.N. Wistisen^a, J. Esberg^b, P. Sona^c, A. Mangiarotti^d, T.J. Ketel^e

^a Department of Physics and Astronomy, Aarhus University, Denmark

^b CERN, Geneva, Switzerland

^c University of Florence, Florence, Italy

^d University of São Paulo, Brazil

^e Free University, Amsterdam, The Netherlands

ARTICLE INFO

Article history:

Received 19 November 2013

Received in revised form 6 March 2014

Accepted 27 March 2014

Available online 2 April 2014

Editor: M. Doser.

Keywords:

Bremsstrahlung

LPM effect

Photon formation length

ABSTRACT

When an ultrarelativistic electron traverses two closely spaced foils, a radiation spectrum ‘resonance’ appears, arising from the photon formation length extending from one foil, across the gap and into the second foil. Several theoretical approaches yield quite different answers to the spectral location of this ‘resonance’, and we have therefore in the CERN NA63 collaboration addressed the question experimentally with a 178 GeV electron beam. The experimental technique used – where a variable gap separates two thin gold foils – allows for a direct measurement of a length that is closely related to the distance over which the photon formation takes place. These are the first measurements to observe the gap dependence of the energy of the ‘resonance’ in the radiation spectrum from a structured target on a truly macroscopic scale up to 0.5 mm. The results are compared with the theory of Baier and Katkov, with both the modified and unmodified theories of Blankenbecler as well as with a naïve, straightforward expectation. Surprisingly, the experiment shows a clear preference for the two latter, comparatively unsophisticated, approaches.

© 2014 The Authors. Published by Elsevier B.V. This is an open access article under the CC BY license (<http://creativecommons.org/licenses/by/3.0/>). Funded by SCOAP³.

1. Introduction

The low-energy radiation emitted by an ultrarelativistic electron traversing a dense medium is suppressed due to the well-known Landau–Pomeranchuk–Migdal (LPM) effect. With a target consisting of two thin, high- Z foils separated by vacuum or a dilute, low- Z material such as air, one can “tune” the suppression by varying the air gap and therefore directly relate the size of the gap to the formation length of the photon by observing at which photon energies, radiation emission is suppressed. Seeing the two foils as one single foil with the central part, which corresponds to the gap, removed, one may expect a suppression–alleviation–suppression effect as the formation length extends into the different regions depending on the photon energy.

An analogy can be made between the radiation emitted by an electron traversing such an above described structured target,

where foils are seen as ‘macroscopic crystalline planes’, and the well-known coherent bremsstrahlung (CB, see, e.g. [1]) emitted by a charged particle interacting with crystalline planes. However, in the former case, the radiation emission from the first foil is only *on the average* in phase with that of the radiation from the second, whereas for interactions in crystals the radiation is to a large extent coherent (barring thermal effects), see also [2]. Furthermore, the main mechanism responsible in the first case is suppression of radiation, contrary to CB, where the effect is coherence. Thus, the ‘resonance’ appearing from closely spaced foils is expected to be much smaller, broader, and at lower energy (reflecting the quite different spacings) than those appearing from CB. Furthermore, whereas the coherence appears over many crystalline planes in coherent bremsstrahlung, due to the averaging mentioned above for the structured target, one can argue that the resonance should disappear when the number of foils in the target is increased. Initial investigations of such many foil targets have been performed and showed no sign of a resonance in the radiation spectrum [3]. Based on this analogy, it could be expected that the measured *location* of the spectral position of these structured target ‘resonances’ –

* Corresponding authors.

E-mail address: ulrik@phys.au.dk (U.I. Uggerhøj).

¹ On sabbatical at: Lawrence Berkeley National Laboratory, Berkeley, USA.

which in the case of coherent bremsstrahlung are in very convincing agreement with theory – would be in good agreement with theory. As this paper aims to show, it is indeed in good agreement with a (semi-)classical, naïve expectation and one theoretical approach, but in clear disagreement with more elaborate theories.

The radiation from an electron traversing a structured target may also seem closely related to transition radiation from a multilayered target, but it is completely different as will be shown in the next section due to the different length scales and energies involved in the two processes. The Lorentz factor times the plasma frequency ω_0 , which is relevant for transition radiation, is much smaller than the photon frequencies relevant in this experiment, and the dielectric properties of the target are therefore not important here.

1.1. The resonance energy

The LPM effect occurs when an ultrarelativistic electron of energy E is deflected by multiple Coulomb scattering outside the typical radiation angle, $\theta_\gamma = 1/\gamma = m_e c^2/E$, within the formation length of the photon. With m_e the electron mass and c the speed of light, the formation length of a photon of frequency ω is

$$l_f(\omega) = \frac{2E(E - \hbar\omega)}{m_e^2 c^3 \omega}, \quad \omega \gg \gamma\omega_0, \quad (1)$$

and when the deflection of the electron is larger than θ_γ over l_f , the radiation emission is suppressed. For energies where the electron recoil is insignificant, $\hbar\omega \ll E$, the formation length is $l_f(\omega) \simeq 2\gamma^2 c/\omega$. Several experiments on the LPM effect have been made over the last 20 years. In particular, a series of experiments at SLAC accurately measured the LPM effect [4,5] and tested the Migdal formula [6], which is a standard within the field. This initiated a significant theoretical interest in the subject by different groups [7–9] who developed new theories, which were more general. The LPM effect has also been investigated at higher energies at CERN [10,11] and for thin targets [3], where the target cannot be considered semi-infinite, as assumed in the Migdal formulation.

In particular, the formulation of Blankenbecler and Drell (BD) [7] can be used in connection with an arbitrary target geometry and Blankenbecler investigated the radiation from a so-called structured target [12], which consists of several targets of equal thickness, l_t , with an equal gap between them, l_g . These calculations predicted a small peak or ‘resonance’ in the radiation spectrum, which has been measured in a previous experiment with two 26 μm gold targets and a 45 μm gap [13]. The results reported in this paper are further discussed in Section 4 since it was subsequently realized that the analysis used was inadequate. The re-analyzed data still shows an indication of a peak in the radiation spectrum which is in agreement with the main claim of the article, but the conclusion about the different theories is changed.

In the two-foil setup, the effect can be seen as a suppression–alleviation–suppression effect caused by multiple Coulomb scattering in the targets. The energies that divide these regions are roughly given by where the formation length is equal to the thickness of the regions, namely l_t and $l_t + l_g$. Here we show new measurements on targets of two 26 μm gold foils with a gap from $l_g = 10 \mu\text{m}$ to 500 μm , which confirm the behavior of the formation length with the photon energy, Eq. (1).

One can also relate the energy at which the LPM suppression begins to the formation length, but it is difficult to define exactly where the suppression enters. Therefore, the structured targets are ideal when one is interested in the connection between l_f and $\hbar\omega$, since they are closely related to $l_g + l_t$ and $\hbar\omega_p$ respectively, where $\hbar\omega_p$ is the energy of the peak. By equating $l_g + l_t$ to l_f , which

corresponds to the photon energy where suppression reappears, one finds

$$\hbar\omega_p = \frac{E}{1 + \frac{m_e c(l_g + l_t)}{2\hbar\gamma}}. \quad (2)$$

One should note that this is not the same condition as for coherent bremsstrahlung, where the formation length may be a factor 2π shorter than the plane-to-plane distance.

Whereas the peak position can be calculated from the full radiation spectra obtained from the theories mentioned above, Baier and Katkov (BK) also give a closed approximate expression for the peak position [14, mentioned below their Fig. 1]. Their expression is

$$\hbar\omega_{p,BK} = \hbar\omega_{th} \frac{l_t}{l_g + l_t}, \quad (3)$$

where $\hbar\omega_{th}$ is the energy where the target becomes thin compared to the formation length. $\hbar\omega_{th}$ is given by $\hbar\omega_{th} = \frac{\hbar\omega_c}{T_c(1+p_c^2)}$ [14, Eq. (3.3)], and can be approximated by $\hbar\omega_{th} \simeq 4\hbar\omega_b = 4\hbar\omega_c/(T_c(1+T_c))$, where $\hbar\omega_c$ is the energy below which the LPM effect becomes significant and is defined below. $T_c = l_t/l_f(\omega_c)$ and $p_c = \gamma\theta_c$ where θ_c is the characteristic radiation angle. In [8] they approximate the characteristic radiation angle θ_c by the characteristic scattering angle θ_s when the scattering is large compared to $1/\gamma$. This approximation, $\theta_c \simeq \theta_s$, is reasonable since the radiation emission angle is of the order $1/\gamma$ and is ‘spread out’ through multiple scattering. Since we are interested in photon energies where the LPM effect is present and scattering therefore is significant, we cannot exclude p_c in the expression for $\hbar\omega_{th}$. Using the standard expression for calculating the multiple scattering angle in one of the gold foils, one obtains $p_c^2 = (\gamma\theta_c)^2 \simeq (\gamma\theta_s)^2 = 4\pi l_t/\alpha X_0 = 13.4$, where X_0 is the radiation length of the target. Using Eq. (2.14) in [14], we find $p_c^2 = 8.8$ for our experimental conditions which is surprisingly different from the previous result.

If one uses the approximation $\hbar\omega_{th} \simeq 4\hbar\omega_b$ as recommended in [14], one obtains the following closed expression for the energy of the peak

$$\hbar\omega_{p,BK} = 4\hbar\omega_c \frac{l_f(\omega_c)^2}{(l_t + l_g)(l_f(\omega_c) + l_t)}, \quad (4)$$

The characteristic energy $\hbar\omega_c$ can conveniently be expressed by [15]

$$\hbar\omega_c = \frac{E^2}{E + 7.68 \text{ TeV/cm} \cdot X_0}, \quad (5)$$

for electrons with energy E in a target with radiation length X_0 . This expression agrees with the expression of BK to within 5% for the relevant situation and is significantly easier to calculate than expression (3.1) in [14]. It is remarkable that Eq. (4) has a $1/l_t^2$ dependence on the target thickness whereas the simple expression Eq. (2) has a $1/l_t$ dependence. Furthermore, if one neglects the p_c term in $\hbar\omega_{th}$, which corresponds to the small scattering limit, one finds in the limit $\hbar\omega_p \ll E$ that the BK expression is identical to Eq. (2). However, as mentioned above, one cannot neglect p_c in our situation and when this is included, the estimate of BK (Eq. (4)) is roughly a factor of 2.3 below Eq. (2) for the present experimental situation. It should be mentioned that in [14] the general condition for the applicability of their theory is $l_t \ll l_c$ where $l_c = l_f(\omega)/(1 + \gamma^2\theta_c^2)$. In our case – even for the 500 μm separation – the relevant parameter l_t/l_c is 0.5 which is not significantly smaller than 1. However, as Baier and Katkov in their paper [14] show calculations for photon energies above 10 MeV, from 25 GeV electrons passing 11.5 μm Au targets, where $l_t/l_c \simeq 0.6$, we

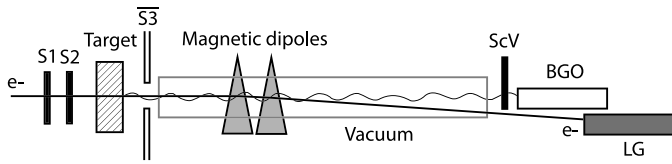


Fig. 1. A schematic drawing of the setup used in the experiment. The beam is defined by three scintillators S1, S2 and S3. Two magnetic dipoles, each 2 meters along the beam, are used at a low field, $B \simeq 0.16$ T, to reduce the influence of synchrotron radiation in the MeV region. This, combined with the necessity of deflecting the electrons outside the BGO calorimeter, into the lead glass (LG) calorimeter, forces a long lever arm. Right in front of the BGO, a veto scintillator, ScV, was mounted to reject events where the photon has converted or events where an electron may have interacted with the vacuum chamber, generating a shower. The total length of the setup was about 70 m [17].

follow their approach that the theory is applicable even in that regime.

Resonance phenomena related to the photon formation length also appear in transition radiation from multilayered targets, but for much lower photon energies $\hbar\omega \ll \gamma\hbar\omega_0$, see e.g. [16]. In this regime the formation length is given by $l_f \simeq 2c\omega/\omega_0^2$ which is significantly different from Eq. (1) in connection to both the photon energy and the Lorentz factor. Furthermore, there is no transition radiation in the exact forward direction, in the absence of scattering.

2. Experiment

The present experiment was performed with the same setup as our measurement of the LPM effect in low- Z targets [17], but with modified targets. Thus, apart from a short introduction and a discussion of the target preparation and distance verification procedures, we refer to [17] for experimental details.

The experiment was performed in the H4 beamline in the North Experimental Area of the Super Proton Synchrotron (SPS) at CERN with a tertiary beam of 178 GeV electrons. This energy was chosen to maximize the formation lengths for the emission of photons with energies in the sensitive range of the bismuth germanate (BGO) calorimeter used, while retaining an acceptable beam intensity.

A schematic drawing of the setup is shown in Fig. 1. The main components are three scintillators used to define the beam, the target assembly and the BGO detector. The emitted photons are detected by the BGO calorimeter which is sensitive from about 100 MeV to 4 GeV, with the settings used. The low-energy limit is determined by synchrotron radiation (SR) and backscatter from the lead glass (LG) detector standing close to the BGO. For more details on the BGO detector the reader is directed to [17].

2.1. Target

The target setup consists of two gold foils of thickness 26 ± 1 μm with a variable gap in between. In this experiment we used gap sizes, l_g , of 10, 60, 100, 200 and 500 μm . One target foil is mounted on a spring-loaded gyro and the other is mounted on a translatable stage. This setup was also used in [13]. The deviations from flatness of the mounted gold foils were checked by laser reflection and found to be less than ± 2 μm . To ensure that the targets were parallel the following method was used. First, the translatable foil was moved toward the gyro-mounted foil and pressed against it, in order for the springs to be slightly compressed and the foils to align. Afterwards, the translatable foil is slowly removed in micrometer steps from the other foil, in order for the gyro-mounted foil to keep its position.

We have determined the gap size by measuring the capacitance between the two targets and reading the position of the translation stage, which is controlled in micrometer steps. In a previous experiment [13] a Mahr MarCator was also used and seen to be in agreement with the readings of the stage controller. To obtain the absolute position we use both the capacitance and the stage position. We assume that the capacitance is equal to a circular parallel-plate capacitor plus an offset. One cannot easily determine the area of the target foils due to the construction of the foil holder, which does not have a sharp edge. Instead, the diameter is adjusted within reasonable limits until a good linear relation with a slope of unity is found between the position calculated from the capacitance and the stage position. We find a diameter of 20.3 ± 0.1 mm which agrees well with the actual size of the target. Accordingly, it is seen that the targets short circuit at a distance of about 9 μm , and since the foils cannot be exactly parallel, it is fair to assume that we can determine the actual gap size with a precision of not more than ± 5 μm in the central region of the target where the beam passes. Obviously, this uncertainty in distance is only important for small gaps (our 10 μm and 60 μm measurements). For large gaps the small uncertainty in position is unimportant since the position of the feature in the radiation spectrum only depends weakly on l_g for large gaps.

3. Simulations

It is necessary to make simulations to compare our data with theoretical models of the radiation spectrum from a structured target. The method used is described in [17] and basically includes a 3% X_0 Bethe–Heitler (BH) background, synchrotron radiation from the bending magnets and radiation from the target calculated with the theories of BD [12,18]. Clearly, as the 2 target foils represent only about 1.6% X_0 , it would be desirable to do the measurements with lower background, but this is challenging in SPS H4 beamline. Increasing the number of foils is also not a solution, since it might make the resonance smaller, as mentioned in the introduction.

We do not track the particles through our setup, and simulate only the radiation emitted. Since we are interested in events where the total energy-loss of the electron is small compared to the electron energy, we can safely neglect electron energy-loss in the simulations. This substantially reduces the computation time. However, since we do not track the particles through the setup, we have to determine a detection efficiency which is mainly due to the veto scintillator positioned in front of the BGO. The efficiency is found by dividing simulations of the background by measurements.

3.1. Target radiation

The radiation spectrum from the structured target is calculated with the theory of BD [7,12] and the modified theory of Blankenbecler (called BD- δ) [18]. They use their eikonal formulation for the wave function and propagate a wave packet through the target taking into account the scattering in the medium, which is modeled as thin, transverse fields with no correlation between the fields. The average transverse momentum acquired over a certain distance is fixed by demanding that the Bethe–Heitler radiation level is reached in the thin target limit. The radiation spectrum is calculated from the electron wave functions given by the eikonal formulation and taking into account the phases which include the effect of the scattering medium. In their first publications [7,12], they include phase changes to order $1/p$ where p is the electron momentum and neglect the changes of the wavefunction amplitude. In the modified theory [18], Blankenbecler treats the scatter-

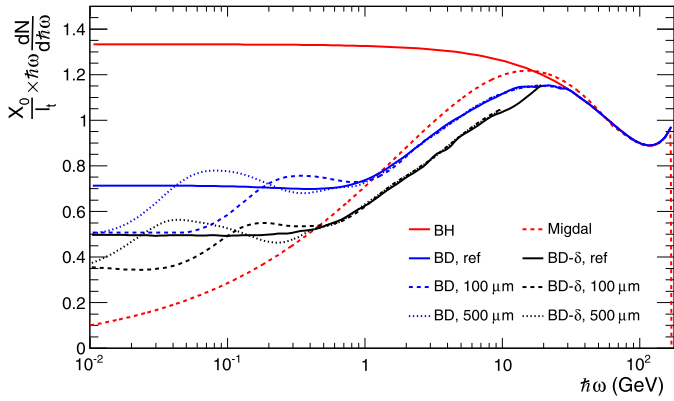


Fig. 2. Calculated radiation power spectra for 178 GeV electrons in gold. The spectra are all normalized to the target thickness, l_t , in units of the radiation length, X_0 . The different curves are described in greater detail in the text. (For interpretation of the references to color in this figure legend, the reader is referred to the web version of this article.)

ing in the medium by functional integration. On the basis of their results in [7] he performs integrations of the form

$$\int [dE_{\perp}] Q[E_{\perp}] \sin \Phi[E_{\perp}], \quad (6)$$

where the functions $Q[E_{\perp}]$ and $\Phi[E_{\perp}]$ can be related to the results of [7]. In this treatment he includes a correlation between the wave function phase and amplitude which has a significant influence on the radiation spectra. It is not clear to us whether or not one can include this phase-amplitude correlation within the eikonal approximation where amplitude changes of order $1/p$ were originally neglected. As seen in the radiation spectra the changes appearing after the modification are quite substantial and a careful experimental investigation can clearly distinguish between them.

The calculated spectra in Fig. 2 show that somewhere below 20 GeV the LPM suppression enters, in accordance with Eq. (5) which gives $\hbar\omega_c \simeq 11.5$ GeV. The red dashed line is the Migdal expression for a semi-infinite target. The formalism of BD naturally incorporates the geometry of the target and therefore also includes effects related to the finite target size. All the blue lines are calculated with the BD formulas and the black lines are calculated with the BD- δ formulas. If the targets are far apart, we do not see any interference effects in the radiation emission and the spectra correspond to two independent and finite targets. In the experiment we use a target separation of 20 mm and call these our reference measurements. The calculated radiation spectra for gap sizes of 100 μm and 500 μm are shown in Fig. 2. These spec-

tra clearly contain a broad peak which moves to lower energies when l_g is increased. For energies below the peak, the spectrum is further reduced to a level below the reference level.

4. Results and discussion

The measured radiation spectra for 3 of our 5 different target spacings are shown in Fig. 3 together with simulations. All spectra include the background which is $\sim 3\%$ X_0 – approximately twice the target thickness (1.6% X_0). The large LPM suppression of the target radiation increases this ratio to 5 to 1 for the reference target at low energies. The LPM effect is not relevant for the background which mainly consists of thin, low- Z materials. The measured spectra are generally in good agreement with simulations. It is worth noting how the radiation spectrum changes with l_g . For the structured target with $l_g = 10$ μm the spectrum does not show a small peak but falls monotonically to a value below the reference spectrum, where the targets are far apart and no interference effects are present. This is similar to the case of a thicker target, since when $l_g < l_t$ the alleviation of the radiation suppression is not significant. To measure ‘resonances’ for even smaller gap sizes would require significantly thinner targets, where background and uncertainties in target flatness would become even greater challenges. When l_g is increased to 60 μm a small peak develops around 700 MeV, and this peak moves to lower energies when l_g is increased.

The effect becomes more pronounced if one plots the ratio between the structured target and the reference target as is done in Fig. 4. The background is subtracted from both spectra. Besides simulations based on the BD formulas, we also plot simulations based on the BD- δ formulas. The same tendencies are seen as those described for the power spectra. The χ^2 values are calculated for the data compared with BD, BD- δ and a constant ratio of unity, which corresponds to no effect. Apart from the 200 μm measurement, where no effect is preferred, our data are consistently in best agreement with the BD theory. However, for the 200 μm measurement, the BD theory is still in good agreement with the data. For the small gaps, constant one can be ruled out and generally the BD- δ is much less probable than the BD theory.

These findings are interesting, since a previous experiment with 197 GeV electrons on structured targets [13] had a preference for the BD- δ theory. After re-analyzing this experiment, it was found that one of the cuts used on the data introduced a significant bias towards low photon energies. When this was corrected, the data were consistent with both the BD, BD- δ and no effect, but with a slight preference for the BD theory. The re-analyzed data are also shown in Fig. 4. Similarly, measurements on thin targets [19] and the LPM effect [17] also have a preference for the BD theory. One is therefore tempted to question the validity of the BD- δ theory.

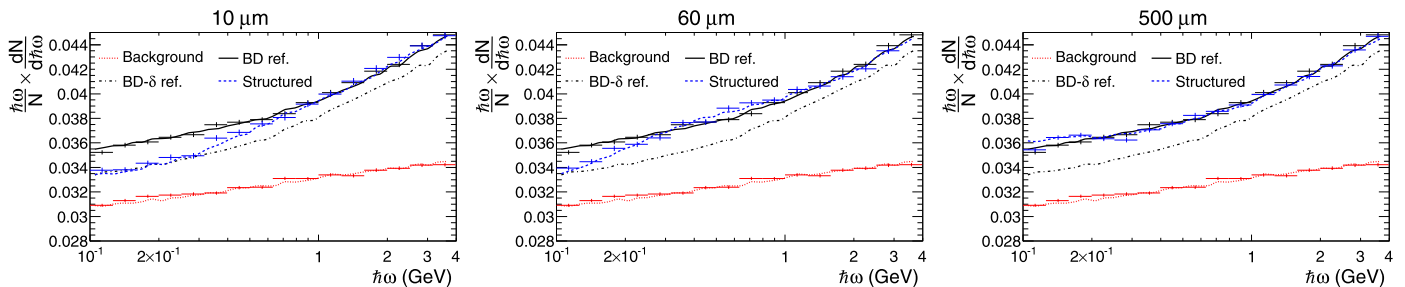


Fig. 3. Radiation power spectra normalized per electron for gap sizes of 10, 60 and 500 μm . The lines are simulations and the markers are data for which the vertical bars indicate the statistical error bars and the horizontal bars are the bin width. The lower red dotted line is the background without the gold foils, the black solid line is the BD reference, the black dash-dot line is BD- δ reference and the blue dashed line is the structured target calculated with the BD formulas. For the reference target, the gold foils are 20 mm apart. (For interpretation of the references to color in this figure legend, the reader is referred to the web version of this article.)

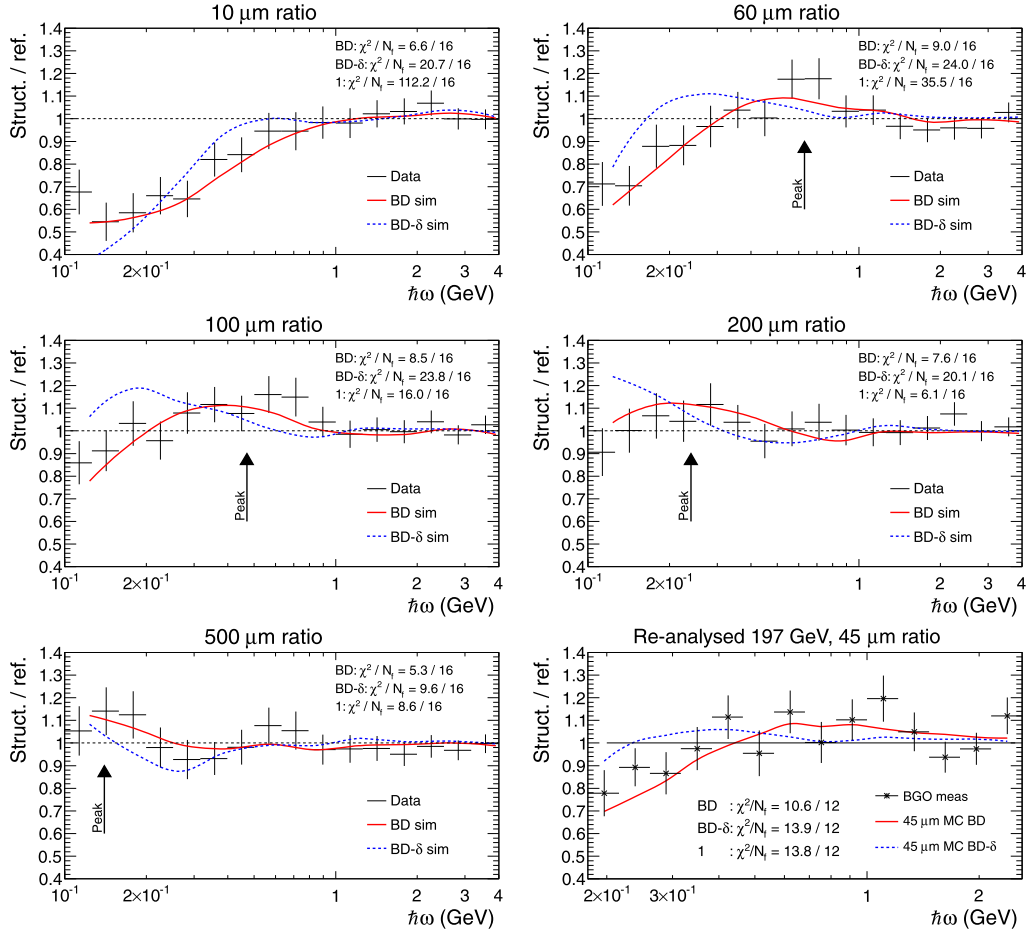


Fig. 4. The ratio between the structured target and the reference target – both with the background subtracted. For the data markers, the vertical bars indicate the statistical error bars and the horizontal bars are the bin width. The solid red lines are simulations based on the BD formulas and the dashed blue lines are based on the BD- δ formulas. The last graph contains the re-analysed data first published in [13]. (For interpretation of the references to color in this figure legend, the reader is referred to the web version of this article.)

From the ratios plotted in Fig. 4 we have determined the position of the peak, $\hbar\omega_p$, by fitting a suitably chosen function of the form

$$f(\hbar\omega) = A \exp\left(\frac{-(\log \hbar\omega - B)^2}{2C^2}\right), \quad (7)$$

in an appropriate interval where A , B and C are fit parameters. It was possible to make a reasonably good fit for $l_g = 60, 100$ and $200 \mu\text{m}$. For $l_g = 10 \mu\text{m}$ no peak is observed and for $l_g = 500 \mu\text{m}$ it was not possible to make a good fit and we have therefore made a simple estimate of $\hbar\omega_p$ from the shape of the data. Furthermore, we have to correct the peak position for the offset caused by backscplash from the LG (see [17] for more details). Basically, all low-energy events are accompanied by a high-energy electron which causes a backscplash from the LG in the BGO and increases the energies by $8 \pm 1 \text{ MeV}$. This is mainly relevant for the largest gaps. The corrected results are plotted in Fig. 5 together with the estimate by Eq. (2), shown as the red line. The agreement is good, which establishes the connection between the formation length of the photon and the position of the peak in the radiation spectrum. For the BD theory the agreement is also good, as expected from the earlier figures, and the peak is positioned at energies substantially higher than for the BD- δ theory. The estimate of BK, Eq. (4), is roughly a factor of 2.3 below Eq. (2) and significantly below our data. The agreement of BK with the BD- δ theory is probably accidental, since the estimate agrees with the BD calculations in other

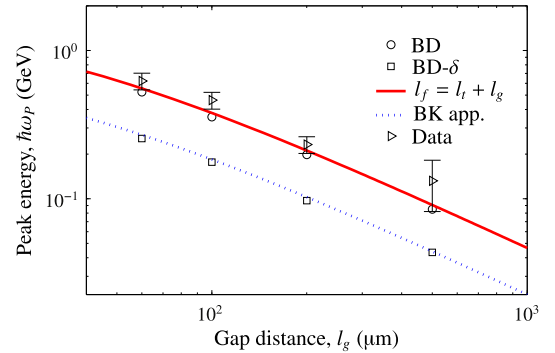


Fig. 5. The position of the peak in the radiation spectrum as a function of the gap size l_g . The red line is Eq. (2) and the blue dashed line is Eq. (4). (For interpretation of the references to color in this figure legend, the reader is referred to the web version of this article.)

cases [14]. This is at least partially due to a $1/l_t^2$ dependence for $\hbar\omega_{p,BK}$ and only $1/l_t$ for $\hbar\omega_p$.

5. Conclusion

The present experiment shows a clear excess of radiation at certain energies from a structured target consisting of two thin gold foils positioned at various distances. We have compared the

radiation spectra with Monte Carlo simulations and found a good agreement with the BD theory. We have furthermore extracted the position of the peak and compared that with the expression of the photon formation length and again found a good agreement. In other words we have measured the energy dependence of a length directly proportional to the formation length. Hence, there are now results for low- Z targets [17], thin targets [3] and the present results, which all indicate that the BD- δ theory is a poorer description of experiments than the uncorrected BD theory. Likewise, the simple approach of equating the formation length to the separation between the centers of the foils when determining the location of the structured target 'resonance', compares significantly better to experiment than the approximation of Baier and Katkov.

As a final remark, it is fascinating that the formation length of radiation emission can be measured at distances up to the macroscopic value of 0.5 mm, even though the wavelength of the radiation is barely 10 femtometers.

Acknowledgements

We wish to thank Per Christensen and Poul Aggerholm for technical support with the experimental setup and DAQ system. UIU wishes to thank A. Belkacem – one of the originators of experimental strong field QED at high energies in structured (crystalline) targets – for his kind hospitality and friendly advice during a 'sabbatical' at LBNL.

References

- [1] G. Diambri Palazzi, High-energy bremsstrahlung and electron pair production in thin crystals, *Rev. Mod. Phys.* **40** (1968) 611–631.
- [2] U.I. Uggerhøj, The interaction of relativistic particles with strong crystalline fields, *Rev. Mod. Phys.* **77** (4) (2005) 1131–1171, <http://dx.doi.org/10.1103/RevModPhys.77.1131>.
- [3] H.D. Thomsen, J. Esberg, K.K. Andersen, M.D. Lund, H. Knudsen, U.I. Uggerhøj, P. Sona, A. Mangiarotti, T.J. Ketel, A. Dizdar, S. Ballestrero, S.H. Connell, Distorted Coulomb field of the scattered electron, *Phys. Rev. D* **81** (5) (2010) 052003, <http://dx.doi.org/10.1103/PhysRevD.81.052003>.
- [4] P.L. Anthony, R. Becker-Szendy, P.E. Bosted, M. Cavalli-Sforza, L.P. Keller, L.A. Kelley, S.R. Klein, G. Niemi, M.L. Perl, L.S. Rochester, J.L. White, An accurate measurement of the Landau-Pomeranchuk-Migdal effect, *Phys. Rev. Lett.* **75** (10) (1995) 1949–1952, <http://dx.doi.org/10.1103/PhysRevLett.75.1949>.
- [5] P.L. Anthony, R. Becker-Szendy, P.E. Bosted, M. Cavalli-Sforza, L.P. Keller, L.A. Kelley, S.R. Klein, G. Niemi, M.L. Perl, L.S. Rochester, J.L. White, Bremsstrahlung suppression due to the Landau-Pomeranchuk-Migdal and dielectric effects in a variety of materials, *Phys. Rev. D* **56** (3) (1997) 1373–1390, <http://dx.doi.org/10.1103/PhysRevD.56.1373>.
- [6] A.B. Migdal, Bremsstrahlung and pair production in condensed media at high energies, *Phys. Rev.* **103** (6) (1956) 1811–1820, <http://dx.doi.org/10.1103/PhysRev.103.1811>.
- [7] R. Blankenbecler, S.D. Drell, Landau-Pomeranchuk-Migdal effect for finite targets, *Phys. Rev. D* **53** (11) (1996) 6265–6281, <http://dx.doi.org/10.1103/PhysRevD.53.6265>.
- [8] V.N. Baier, V.M. Katkov, Theory of the Landau-Pomeranchuk-Migdal effect, *Phys. Rev. D* **57** (5) (1998) 3146–3162, <http://dx.doi.org/10.1103/PhysRevD.57.3146>.
- [9] B.G. Zakharov, Landau-Pomeranchuk-Migdal effect for finite-size targets, *Pis'ma Zh. Eksp. Teor. Fiz.* **64** (1996) 737, <http://dx.doi.org/10.1134/1.567248>, arXiv:hep-ph/9612431.
- [10] H.D. Hansen, U.I. Uggerhøj, C. Biino, S. Ballestrero, A. Mangiarotti, P. Sona, T.J. Ketel, Z.Z. Vilakazi, Is the electron radiation length constant at high energies?, *Phys. Rev. Lett.* **91** (1) (2003) 014801, <http://dx.doi.org/10.1103/PhysRevLett.91.014801>.
- [11] H.D. Hansen, U.I. Uggerhøj, C. Biino, S. Ballestrero, A. Mangiarotti, P. Sona, T.J. Ketel, Z.Z. Vilakazi, Landau-Pomeranchuk-Migdal effect for multihundred GeV electrons, *Phys. Rev. D* **69** (3) (2004) 032001, <http://dx.doi.org/10.1103/PhysRevD.69.032001>.
- [12] R. Blankenbecler, Structured targets and the Landau-Pomeranchuk-Migdal effect, *Phys. Rev. D* **55** (1) (1997) 190–195, <http://dx.doi.org/10.1103/PhysRevD.55.190>.
- [13] K.K. Andersen, et al., Direct measurement of the formation length of photons, *Phys. Rev. Lett.* **108** (2012) 071802, <http://dx.doi.org/10.1103/PhysRevLett.108.071802>.
- [14] V.N. Baier, V.M. Katkov, Landau-Pomeranchuk-Migdal effect and transition radiation in structured targets, *Phys. Rev. D* **60** (7) (1999) 076001, <http://dx.doi.org/10.1103/PhysRevD.60.076001>.
- [15] S. Klein, Suppression of bremsstrahlung and pair production due to environmental factors, *Rev. Mod. Phys.* **71** (5) (1999) 1501–1538, <http://dx.doi.org/10.1103/RevModPhys.71.1501>.
- [16] X. Artru, G.B. Yodh, G. Mennessier, Practical theory of the multilayered transition radiation detector, *Phys. Rev. D* **12** (5) (1975) 1289, <http://dx.doi.org/10.1103/PhysRevD.12.1289>.
- [17] K.K. Andersen, S.L. Andersen, J. Esberg, H. Knudsen, R.E. Mikkelsen, U.I. Uggerhøj, T.N. Wistisen, P. Sona, A. Mangiarotti, T.J. Ketel, Experimental investigation of the Landau-Pomeranchuk-Migdal effect in low- z targets, *Phys. Rev. D* **88** (2013) 072007, <http://dx.doi.org/10.1103/PhysRevD.88.072007>.
- [18] R. Blankenbecler, Multiple scattering and functional integrals, *Phys. Rev. D* **55** (4) (1997) 2441–2448, <http://dx.doi.org/10.1103/PhysRevD.55.2441>.
- [19] H.D. Thomsen, Taming GeV photons and antimatter, Ph.D. thesis, Aarhus University, 2010.